Electron paramagnetic resonance of the $[Be]^+$ centre in MgO:Be

2003 J. Phys.: Condens. Matter 15 6871

(http://iopscience.iop.org/0953-8984/15/40/022)

INSTITUTE OF PHYSICS PUBLISHING JOURNAL OF PHYSICS: CONDENSED MATTER

J. Phys.: Condens. Matter **15** (2003) 6871–6878 PII: S0953-8984(03)66053-4

Electron paramagnetic resonance of the $[Be]^+$ centre in MgO:Be

S A Dolgov[1], V Isakhanyan[2], T Kärner[1,3], A Maaroos[1] and S Nakonechnyi[2]

[1] Institute of Physics, University of Tartu, Riia 142, 51014 Tartu, Estonia
[2] University of Tartu, Ülikooli 18, 51014 Tartu, Estonia

E-mail: tiit@fi.tartu.ee (T Kärner)

Received 10 July 2003
Published 26 September 2003
Online at stacks.iop.org/JPhysCM/15/6871

Abstract

In Be-doped MgO crystals, a new hole centre has been discovered whose physical properties are similar to those of $[Li]^0$-type centres (a hole localized at a cation impurity). The centre can be observed best by electron paramagnetic resonance (EPR) at liquid He temperature; thermal destruction of the centre through the loss of a hole takes place at about 160 K. The symmetry of the centre is almost tetragonal, with a slight rhombic distortion, and the hyperfine structure of its EPR spectrum suggests the following model for the centre: Be^{2+}–O^-. However, a detailed investigation of the temperature dependence of the EPR spectrum did not reveal, contrary to our preliminary announcement, any temperature averaging. At higher temperatures the spectrum is complicated by the wealth of spectral lines induced by the ubiquitous Be impurity ions. In particular, this led to our former misinterpretation. The physical properties of the observed centre are discussed and compared with those of analogous centres in MgO.

1. Introduction

It is generally accepted that self-trapping of holes does not take place in MgO. However, holes are easily trapped on the oxygen ions located adjacent to cation vacancies (the so-called V-type centres: V^-, V^0, V_{OH}, V_F, V_{Al}) or monovalent cations ($[Li]^0$, $[Na]^0$ centres, the upper index shows the effective charge of the centre). The excess negative charge of the V centres (except V^- centres) is compensated by various aliovalent impurities at the neighbouring anion or cation sites. An overview of the properties of these hole centres can be found in [1, 2].

To understand the hole trapping process in MgO, and especially the absence of self-trapping, it is instructive to investigate the trapped hole centres, where an interaction between

[3] Author to whom any correspondence should be addressed.

the trapped hole and the adjacent cation is not mainly electrostatic but is due to the deformation of the crystal lattice caused by the hole. This means that instead of trapped hole centres with monovalent cations we should investigate those centres with divalent, preferably isoelectronic, cations.

Such a centre, namely $[Mg]^+$, has been found using electron paramagnetic resonance (EPR) in SrO [3]. The symmetry of the centre at $T < 20$ K was nearly tetragonal, with a slight rhombic distortion. The main axis (Z) of the centre, as well as the X-axis, lies in a $\{100\}$ plain and was tilted by about 1° in relation to a $\langle 100 \rangle$ crystal direction. The Y-axis coincides with a $\langle 100 \rangle$ crystal axis. At $T > 20$ K the EPR spectrum of the centre starts to change and at $T > 50$ K the spectrum of the centre is tetragonal. Such behaviour was assigned to a hopping movement of the non-central Mg^{2+} ion between possible non-equivalent positions in a cation lattice site.

Another possible detection of an isoelectronic hole centre in the simple oxide, namely a $[Ca]^+$ centre in MgO, has been reported in [4, 5]. A 6.8 eV luminescence band and a 48 K thermoluminescence peak, observed in Ca-doped MgO crystals, were related to the luminescence of small-radius excitons trapped by the Ca cation impurity and to a thermal release of the holes trapped by Ca, respectively. However, this model has not been confirmed by independent EPR measurements of MgO:Ca crystals irradiated with x-rays at a low (<20 K) temperature. Possible reasons for this failure will be discussed at the end of this paper.

In this paper we report the results of the EPR investigation of a hole centre in Be-doped MgO, presumably $[Be]^+$. Our preliminary announcement about this centre [6, 7] contained an erroneous statement about the motional averaging of the EPR spectrum of this centre at $T > 30$ K. A later careful investigation showed, however, that this was not true: the spectral lines that were taken for the averaged spectrum did not belong to this centre.

2. Experimental details

The MgO:Be single crystals were grown at the Institute of Physics, University of Tartu, by a variation of an arc fusion technique [8]. Details of the crystal growth were described in [6]. As a result, crystals up to $15 \times 15 \times 10$ mm^3 were formed. An average content of the most common transition metal impurities in these crystals was about 10 ppm. In MgO, Be^{2+} substitutes Mg^{2+}, and was found to be present both in the form of isolated ions and as a part of defect complexes. The estimated content of Be in the MgO:Be crystals was about 100 ppm. The EPR spectra were measured with an X-band (9.928 GHz) ERS 231 spectrometer. A continuous-flow helium cryostat (Oxford Instruments, ESR900) was used to keep the samples at the necessary temperature. Pulse annealing of the samples was carried out to determine the thermal stability of the observed EPR-active centres. On pulse annealing, after rapid heating up, the crystals were kept for 2 min at the required temperature and then cooled down to the measurement temperature. The measured EPR spectra were analysed using the computer program EPR-NMR (Department of Chemistry, University of Saskatchewan, Canada, 1993).

3. Experimental results

When MgO:Be crystals are subjected to x-irradiation, new paramagnetic centres are formed. One of them—the V_{OH-Be} centre (linear defect Be^{2+}–O^-–v_c–OH^-)—was described in [6]. It was shown that the physical properties of this centre differ significantly from those of a 'usual' V_{OH} centre. Besides the V_{OH-Be} centre and the V_{OH} centre, EPR spectra of the centres whose physical properties (g-factor, temperature dependence etc) resemble those of the V_{OH} centre

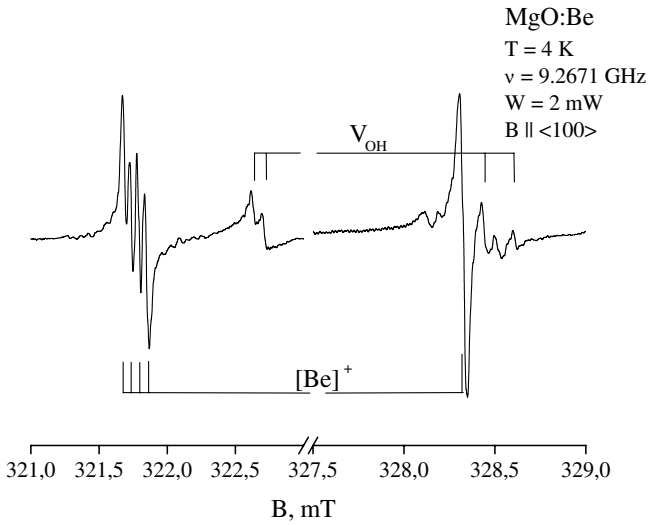

Figure 1. EPR spectrum of $[Be]^+$ centres at 4 K. The external magnetic field $\boldsymbol{B}$ is oriented along a ⟨100⟩ crystal direction. In addition to the $[Be]^+$ spectrum, the lines of a heavily saturated V_{OH} centre are visible.

but show a characteristic Be hyperfine structure can be observed. The intensity of these lines is about an order lower than the intensity of V_{OH} centres. At temperatures $T < 40$ K in the crystals x-irradiated at 77 K, another new EPR spectrum with a four-line superhyperfine (shf) structure becomes observable. Later we shall refer to this centre as a $[Be]^+$ (i.e. $Be^{2+}O^-$) centre. The validity of this assumption will be proved below. The paramagnetic resonance spectrum of this centre can be followed in the temperature range of 4–40 K and is best observed at 4 K and at high microwave powers (>1 mW) when the EPR spectra of all other paramagnetic centres are already saturated. The EPR spectrum of the $[Be]^+$ centre measured at 4 K after x-irradiation of the crystal at 77 K, at the orientation of the magnetic field $\boldsymbol{B}$ parallel to a ⟨100⟩ crystal axis, is shown in figure 1. At this particular orientation the spectrum consists of a low-field group of four lines, and a single high-field line. The distance between the lines in the group is about 0.055 mT. In addition to the spectral lines mentioned above, heavily saturated lines of the V_{OH} centre are visible. The position of these lines was used as a benchmark to determine the g-factor of the centre and the orientation of the crystal in an external magnetic field $\boldsymbol{B}$.

The angular dependence of the EPR spectrum is shown in figure 2. The magnetic field lies in a {001} plane; α is the angle between the magnetic field direction and a ⟨100⟩-type crystal axis. The solid curves represent the calculated angular dependence, the line positions used later in the fitting process are depicted as open circles. At most crystal orientations the spectral lines were not resolved and their positions could not be measured exactly.

For a general orientation of the magnetic field $\boldsymbol{B}$ in this plane, the spectrum consists of six groups of lines, consistent with the orthorhombic symmetry of the centre. However, the deviation from a tetragonal symmetry is quite small. Each group, in its turn, consists of four lines. The relative positions of the lines in these groups depend on the orientation of the crystal in the external magnetic field. The width of the spectral lines within a group ($\sim$0.03 mT) is of the same order of magnitude as the distance between the lines. For that reason, it is difficult to determine the widths of the individual spectral lines at higher temperatures when the lines begin to broaden.

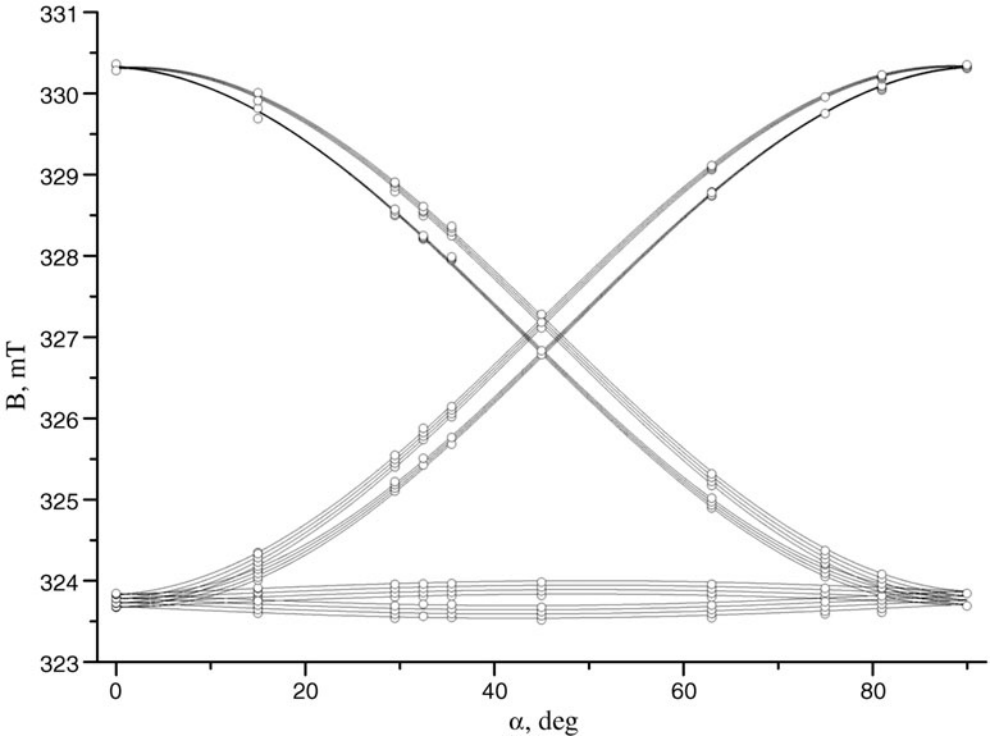

Figure 2. Angular dependence of the $[Be]^+$ EPR spectrum, calculated (solid curves) and experimental points. The magnetic field lies in a {001} plane, α is the angle between magnetic field direction and a ⟨100⟩ crystal axis.

In figure 3, the dependence of the intensity of the EPR spectrum on the measuring temperature is given. When the measuring temperature rises, the intensity of the spectrum declines abruptly and at the same time the EPR signal of the V_{OH} centre and its associated low-field four-line structure, mentioned above, rapidly increases. At ∼15 K the spectrum of the V_{OH} centre is clearly the dominant one. Our provisional and erroneous conclusion about a motional averaging of the spectrum at higher temperatures was due to a confusion of spectral lines belonging to different centres. Although we could not measure the temperature dependence of the EPR spectrum line widths of the $[Be]^+$ centre, it seems that they grow monotonically until the complete disappearance of the EPR signal at about 60 K. The thermal destruction of the centre, however, takes place at a much higher temperature.

The thermal stability of the investigated centre in an MgO:Be crystal x-irradiated at 77 K was measured using pulse annealing and is also shown in figure 3. In this figure the change of the intensity of the V_{OH} centre is also depicted. It can be seen that at the temperature of the disappearance of the centre, a growth in the number of V_{OH} centres takes place.

4. Discussion

4.1. Spin Hamiltonian parameters and model of the centre

The nucleus with $I = 3/2$ that gives rise to the observed four-line hyperfine structure of the spectrum is obviously the doped ^{9}Be. The g-factor of the centre is bigger than g-factor of the

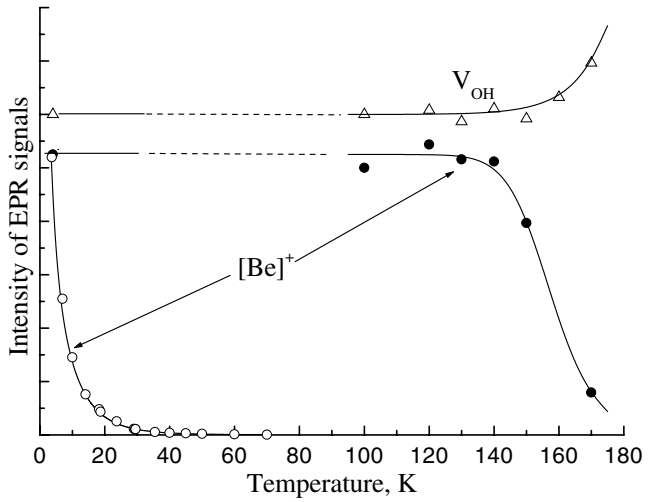

Figure 3. Temperature dependence of the intensity of the $[Be]^+$ EPR spectrum (open circles) and variation of EPR signals of $[Be]^+$ (measured at 4 K, solid circles) and V_{OH} centres (measured at 80 K, open triangles), as a result of heating to temperatures, corresponding to experimental points, and subsequent recooling (isochronal annealing). Solid curves are guides for eye.

free electron, which points to a hole centre. The almost tetragonal symmetry of the centre and the magnitude of the hyperfine splitting that is close to the Be-induced splitting in the V_{OH-Be} centre show that the structure of this centre is similar to the corresponding part of the V_{OH-Be} centre. Therefore, we attribute the observed spectrum to a linear defect that we, in analogy to the well-known $[Li]^0$ or $[Na]^0$ centres in MgO, refer to as a $[Be]^+$ centre: Be^{2+}–O^-.

The EPR spectrum and its angular dependence can be described using the following spin Hamiltonian:

$$H = \beta \boldsymbol{S}\boldsymbol{g}\boldsymbol{B} + h\boldsymbol{S}\boldsymbol{A}_{\mathrm{Be}}\boldsymbol{I}_{\mathrm{Be}} - g_{\mathrm{Be}}\beta_{\mathrm{N}}\boldsymbol{B}\boldsymbol{I}_{\mathrm{Be}},$$

where $S = 1/2$ and $I_{\mathrm{Be}} = 3/2$. The first term describes the electron Zeeman interaction, the second the shf interaction and the third term the nuclear Zeeman interaction. The term describing nuclear quadrupole interaction was found to be insignificant and was not included.

Assuming a rhombic symmetry of the centre, a least-squares fitting of the calculated spectrum to the experimental data gave the following parameters of the spin Hamiltonian: $g_X = 2.0465 \pm 0.0002$, $g_Y = 2.0447 \pm 0.0002$, $g_Z = 2.0045 \pm 0.0002$, $A_{\mathrm{Be}X} = 1.64 \pm 0.05$ MHz, $A_{\mathrm{Be}Y} = 1.49 \pm 0.05$ MHz, $A_{\mathrm{Be}Z} = 0.08 \pm 0.05$ MHz. Here we have written the main values both g and A tensors in a common system of main axes XYZ. Actually the fitting procedure gave slightly different values for the orientation of the main axes of the A tensor compared with those of the g tensor. However, because of a small difference in the orientation of these axes and a comparatively low accuracy in the determination of values of the A tensor, these axes may be regarded as coincident. The orientation of the XYZ axes in relation to the crystal axes is as follows: the X-axis coincides with a $\langle 110 \rangle$ crystal direction; the Z and X axes lie in a $\{110\}$ plane and are deflected by 2.42° from, respectively, $\langle 001 \rangle$ and $\langle 1\bar{1}0 \rangle$ directions. The symmetry group of the defect contains besides the identity operation the reflection about a $\{110\}$ plane and is C_S. Taking into account that the symmetry of a regular lattice site in MgO is O, it gives 24:2 = 12 non-equivalent possible orientations of the defect with respect to the orientation of the external magnetic field $\boldsymbol{B}$. If the magnetic field lies in a $\{100\}$ plane, as in our case, the number of different spectra is reduced to six (see figure 2). Hence, the symmetry

Table 1. A comparison of the physical properties of hole centres in MgO.

Centre	$\Delta g = g_\perp - g_e$	a (MHz)	b (MHz)	Ion–hole distance d (nm)	Temperature of thermal destruction (K)
$[Be]^+$	0.0442	$+1.07 \pm 0.05$	-0.494 ± 0.033	0.299 ± 0.030	160 ± 5
$[Li]^0$	0.0519 [1]	−4.80 [1]	+2.12 [3]	0.247 [10]	230 [11]
$[Na]^0$	0.0698 [1]	−8.61 [1]	+2.79 [3]	0.186 [10]	190 [12]
V_{OH-Be}	0.0227 [6]	+1.34[a] [6]	−0.67[a] [6]	0.271[a]	400 [6]
		0.353[b] [6]	2.432[b] [6]	0.332[b]	
V_{OH}	0.0373 [1]	0.101 [1]	2.371 [1]	0.334	335 [11]

[a] Be ion.
[b] H ion.

of the $[Be]^+$ centre differs from the symmetry of the $[Mg]^+$ centre in SrO [3] where one axis of the centre was directed along a ⟨100⟩ crystal direction, two others lying in a {100} plane, but it is exactly the same as reported in [9] for a Cu^{2+} ion in SrO. In both those cases a motional averaging of the spectrum at $T > 10$ K was observed.

4.2. Physical properties of the [Be]$^+$ centre

It is instructive to compare the obtained results with the corresponding properties of the other hole centres in MgO. Table 1 gives some spin Hamiltonian parameters for a number of hole centres, the g-factor shift from free electron value, isotropic and anisotropic shf splitting constants (a and b, respectively), values calculated from them, namely impurity ion–hole distances and measured thermal destruction temperatures of the centres.

The values of the g-factor shift reflect the energy between the ground and the first excited energy level ΔE of the defect centre: $\Delta g \approx -2\lambda/\Delta E$, where λ is the spin–orbit coupling parameter [1]. In the first approximation ΔE is determined by the value of an axial crystal field at the hole position. If our models of the V_{OH-Be} and $[Be]^+$ centres are correct, then the V_{OH-Be} centre Be^{2+}–O^-–v_c–OH^- can be regarded as a sum of $[Be]^+$ and V_{OH} centres and the axial crystal field in the O^- ion position is the sum of the contributions from $[Be]^+$ and V_{OH} parts of a V_{OH-Be} centre. Therefore, $1/\Delta g(V_{OH-Be}) \approx 1/\Delta g([Be]^+) + 1/\Delta g(V_{OH})$. Using the values of Δg from table 1, we get $44.9 \approx 27.0 + 22.6$ that is an acceptable result taking into account the approximations we made, and supports the models of the centres.

The increase of the Δg in the row V_{OH-Be}–V_{OH}–$[Be]^+$–$[Li]^0$–$[Na]^0$ reflects the decrease of the various terms contributing to the axial crystal field: a cation vacancy, a monovalent impurity in the cation site, an electric dipole due to the shifted position of the small Be^{2+} ion in the cation site. It is interesting that the last term clearly outweighs the Coulombic contribution connected with the monovalent Li^+ and Na^+ impurities: the g-factor shift for the $[Be]^+$ centre is considerably smaller than for the $[Li]^0$ centre. (Six-coordinated ionic radii of Mg^{2+} and Li^+ are almost equal—0.086 and 0.090 nm, respectively, the one for Be^{2+} ion considerably lower −0.059 nm [13].)

Through the Kronig–Van Vleck mechanism, the time of spin–lattice relaxation is related to the ΔE and g factor shift: the bigger the shift, the lower the most suitable temperature to observe the EPR spectra of the centre. The EPR spectrum of the V_{OH-Be} centres could be observed only at $T > 40$ K, and at a moderate microwave power of about 1 mW the best temperature to record the EPR spectra was room temperature. The EPR signal of the V_{OH} centres at the same conditions saturates at $T < 15$ K and begins to broaden at $T > 80$ K. The

best temperature to record the EPR signal of the [Be]$^+$ centres was 4 K, this also holds for [Li]$^+$ and, especially, [Na]$^+$ centres.

The thermal destruction of these hole centres takes place through a thermal release of the trapped hole. The temperature of this process is determined by the depth of the whole potential well, not only by the axial part of the crystal field as in the case of Δg. As one can see from the table, the temperature of thermal destruction is indeed lower for the [Be]$^+$ centre, where the potential well is created by the relaxation of the surrounding ions only, than for the Li and Na containing centres with an effective Coulombic charge.

The values of the isotropic and anisotropic shf constants of the [Be]$^+$ centre are as follows: $a_{\mathrm{Be}} = 1.07$ MHz, $b_{\mathrm{Be}} = -0.494$ MHz. As it has been repeatedly observed for the [Li]^0-type of centres (but not for V centres), the shf constants have different signs, the apparent spin density at the impurity nucleus (that enters as a multiplier into the isotropic shf term) being negative [11, 14]. Just the same holds in our case (notice that the nuclear g-factor of Be is negative; as a result, the signs of a and b are reversed). Comparison a_{Be} with the isotropic hyperfine interaction constant for the unit spin density in the Be 2s orbital (451.6 MHz [15]) shows that the admixture of this orbital into the defect wavefunction is very low. This is consistent with the tight binding of the hole localized near a cation impurity. On this basis, and taking into account the $1s^2$ electron configuration of a Be^{2+}, it is justified to consider the anisotropic shf interaction as a distant point dipole–dipole interaction. Using the found b value, the distance between the nucleus and the hole can be estimated ($b = 95.625 g_{\mathrm{N}}/r^3$ [16], where b is given in megahertz where g_{N} is the nuclear g-factor and the distance r is calculated in atomic units). This calculation can be improved further, using the formula $1/r^3 = 1/d^3 + 12\langle\rho^2\rangle/(5\mathrm{d}^3)$ [14] that takes into account the finite extension of the p orbital of the hole. The distances d calculated in such a way are given in table 1. These distances should be compared with the MgO lattice constant of $a_0 = 0.42$ nm (or the interionic distance $a_0/2 = 0.21$ nm). As we can see, the calculated distance between the nucleus and the hole, 0.299 nm $\approx 1.4\ a_0/2$, is considerably bigger than the interionic distance. This reflects the outward relaxation of Be^{2+} and O^- ions. However, it is also bigger than the corresponding distance in a $V_{\mathrm{OH-Be}}$ centre ($1.2\ a_0$). This result is expected if we take into account that in a V centre an outward relaxation of the hole from a cation vacancy takes place. In a $V_{\mathrm{OH-Be}}$ centre this relaxation tries to shift the hole towards the Be^{2+} ion; in a [Be]$^+$ centre there is no cation vacancy and no corresponding relaxation.

Consequently, in the [Be]$^+$ centre as well as in the $V_{\mathrm{OH-Be}}$ centre, the Be^{2+} ion is shifted far away from the centre of the cation vacancy. Additionally, in the case of the [Be]$^+$ centre we can say that this shift occurs in a $\{110\}$ plane, presumably along a $\langle 111\rangle$ direction into an almost interstitial position. This may be the reason why we do not observe any hopping movement of the Be^{2+} ion. A further investigation may clarify this question.

Finally, the experience of EPR investigation of these hole centres can tell us why the EPR signal of [Ca]$^+$ centres in MgO has not yet been found (if they do exist). It can be supposed that one should look for it in the MgO:Ca crystals at $T < 4$ K using a relatively high (>10 mW) microwave power presumably at the region of g-factors 2.05–2.10. The crystals must be irradiated (and kept before the measurements) at $T < 30$ K.

5. Conclusions

In Be-doped MgO crystals under x-irradiation at $T < 80$ K a new hole centre—a hole trapped by an impurity Be^{2+} ion, isoelectronic with Mg^{2+}, ([Be]$^+$ centre)—is formed. The [Be]$^+$ centre is the closest analogue to a self-trapped hole in MgO so far investigated by EPR. The Be^{2+} ion substitutes a Mg^{2+} cation but because of its significantly smaller ionic radius (0.059 nm

against 0.086 nm for Mg^{2+}) it is shifted along a ⟨111⟩ crystal direction. All the results of EPR measurements confirm this model, however, contrary to some other analogous centres, in the range of temperatures where the spectrum is still observable (up to 60 K) we did not observe a motional averaging of its EPR spectrum due to a hopping movement of the Be^{2+} ion between its non-equivalent positions.

Acknowledgment

This work was supported by the Estonian Science Foundation (grant no 5027).

References

[1] Henderson B and Wertz J E 1977 *Defects in the Alkaline Earth Oxides* (London: Taylor and Francis)
[2] Chen Y and Abraham M M 1990 *J. Phys. Chem. Solids* **51** 747
[3] Lehto T P, Seeman V O and Haldre J J 1984 *Fiz. Tverd. Tela* **26** 3042
[4] Feldbakh E Kh, Lushchik Ch B and Kuusmann I L 1984 *JETP Lett.* **39** 61
[5] Kärner T, Malysheva A F and Tazhigulov B 1984 *Trudy IF Akad. Nauk Est. SSR* **55** 217 (in Russian)
[6] Dolgov S A, Isakhanyan V, Kärner T, Maaroos A and Nakonechyi S 2002 *J. Phys.: Condens. Matter* **14** 8881
[7] Kärner T, Dolgov S A, Isakhanyan V, Maaroos A and Nakonechyi S 2003 *Radiat. Eff. Defects Solids* **158** 163
[8] Maaroos A 1982 *Trudy IF Akad. Nauk Est. SSR* **53** 49 (in Russian)
[9] Tolparov Yu N, Bir G L, Sochava L S and Kovalev N N 1974 *Fiz. Tverd. Tela* **16** 895
[10] Abraham M M, Unruh W P and Chen Y 1974 *Phys. Rev.* B **10** 3540
[11] Kärner T, Malysheva A F, Maaroos A and Mürk V V 1980 *Sov. Phys.—Solid State* **22** 1178
[12] Abraham M M, Chen Y, Kolopus J L and Tohver H T 1972 *Phys. Rev.* B **5** 4945
[13] Shannon R D 1976 *Acta Crystallogr.* A **3** 759
[14] Schirmer O F 1971 *J. Phys. Chem. Solids* **32** 499
[15] Morton J R and Preston K F 1978 *J. Magn. Reson.* **30** 577
[16] Spaeth J M, Niklas J R and Bartram R H 1992 *Structural Analysis of Point Defects in Solids* (*Springer Series in Solid-State Sciences*) (New York: Springer)